A conserved uORF impacts APOBEC3G translation and is essential for translational inhibition by the HIV-1 Vif protein

Camille Libre[1,#], Tanja Seissler[1,#], Santiago Guerrero[1], Julien Batisse[1], Cédric Verriez[1], Benjamin Stupfler[1], Orian Gilmer[1], Melanie M. Weber[1], Andrea Cimarelli[2], Lucie Etienne[2], Roland Marquet[1] & Jean-Christophe Paillart[1,*]

[1]Université de Strasbourg, CNRS, Architecture et Réactivité de l'ARN, UPR 9002, 2 Allée Conrad Roentgen, F-67084 Strasbourg cedex, France

[2]CIRI-International Center for Infectiology Research, INSERM U1111, Université Claude Bernard Lyon 1, CNRS, UMR5308, Ecole Normale Supérieure de Lyon, Université Lyon, F-69000 Lyon, France

*To whom correspondence should be addressed: Tel: (+33) (0)3 88 41 70 35; Fax: (+33) (0)3 88 60 22 18; E-mail: jc.paillart@ibmc-cnrs.unistra.fr

[#] The authors wish it to be known that, in their opinion, the first two authors should be regarded as joint First Authors

Present address:

- Libre: CellVax, SAS, Villejuif BioPark, 1 Mail du Prof. Georges Mathé, F-94800 Villejuif, France
- Seissler: Novartis, Fabrikstrasse 2, 4056 Basel, Switzerland
- Guerrero: Centro de Investigación Genética y Genómica, Facultad de Ciencias de la Salud Eugenio Espejo, Universidad UTE, 170129 Quito, Ecuador.
- Batisse: IGBMC, Université de Strasbourg, CNRS UMR 7104, INSERM U1258, F-67404 Illkirch-Graffenstaden cedex, France
- Weber: Julius-Maximilians-Universität Würzburg, Sanderring 2, 97070 Würzburg, Germany

ABSTRACT

The HIV-1 Vif protein is essential for viral fitness and pathogenicity. Vif decreases expression of cellular cytosine deaminases APOBEC3G (A3G), A3F, A3D and A3H, which inhibit HIV-1 replication by inducing hypermutations during reverse transcription. Vif counteracts A3G by several non-redundant mechanisms (transcription, translation and protein degradation) that concur in reducing the levels of A3G in cell and in preventing its incorporation into viral particles. How Vif affects A3G translation remains unclear. Here, we uncovered the importance of a short conserved uORF (upstream ORF) located within two critical stem-loop structures of the 5' untranslated region (5'UTR) of A3G mRNA. Extensive mutagenesis of A3G 5'-UTR, combined with an analysis of their translational effect in transfected cells, indicated that the uORF represses A3G translation and that A3G mRNA is translated through a dual leaky-scanning and re-initiation mechanism. Interestingly, the uORF is also mandatory for the Vif-mediated repression of A3G translation. Furthermore, we showed that the redirection of A3G mRNA into stress granules was dependent not only on Vif, but also on the uORF. Overall, we discovered that A3G translation is regulated by a small uORF conserved in the human population and that Vif uses this specific motif to repress its translation.

INTRODUCTION

The Human Immunodeficiency virus (HIV-1) Vif (Viral infectivity factor) protein is essential for production of infectious particles in target cells (1). Indeed, early studies demonstrated that Vif is necessary for virus replication in primary lymphoid and myeloid cells (also called non-permissive cells) but dispensable in a subset of immortalized T cell lines (permissive cells) (2–4). This characteristic is due to the expression of a dominant inhibitor of HIV-1 replication in non-permissive cells (5, 6), later identified as APOBEC3G (Apolipoprotein B mRNA editing enzyme, catalytic polypeptide-like 3) or A3G (7). A3G belongs to a larger family of cytidine deaminases (A3A to A3H) that interfere with reverse transcription by inducing mutations during the synthesis of the viral single-stranded (-) DNA, thus leading to cytidine to uridine transitions and production of non-infectious viral particles (8). Amongst these deaminases, A3D, A3F, A3G and A3H have been shown to efficiently block HIV-1 replication after viral entry (9–14). HIV-1 expresses the non-structural Vif protein to counteract the highly potent intrinsic antiviral activities of A3 proteins, in particular A3F and A3G, which are the most potent against HIV-1 (9, 14, 15). In the absence of Vif, A3G and A3F are packaged into viral particles (16–21) and induce viral DNA hypermutations at the next replication cycle, which in turn results in non-functional viral proteins. Furthermore, there is also evidence that A3G and A3F can inhibit the reverse transcription and the integration steps through a deamination-independent mechanism (22–26). In HIV-1, three distinct and mutually reinforcing mechanisms are employed by Vif to reduce A3G expression and counteract its antiviral activity (27). First, Vif recruits a Cullin-RING E3 ligase 5 (CRL5) complex (composed of the Cullin 5, Elongin B/C, Rbx2, and ARIH2 proteins) to A3 proteins to promote their polyubiquitination and subsequent proteasomal degradation (28–31). This pathway is best characterized (31–34). Secondly, the interaction of the transcriptional cofactor CBF-β (Core Binding Factor β) with Vif-CRL5 affects its association with the RUNX family of transcription factors, leading to the downregulation of RUNX-dependent genes, to which A3G belongs (35, 36). Thirdly, Vif counteracts A3G expression by reducing its translation (37–39). Indeed, we previously showed that two stem-loop structures (SL2-SL3) within the 5'-untranslated region (UTR) of A3G mRNA are essential for the translational inhibition of A3G by Vif (40). Importantly, both proteasomal degradation and translational inhibition of A3G by Vif participate to reduce the intracellular level of A3G and inhibit its packaging into viral particles, demonstrating that HIV-1 has evolved redundant mechanisms to specifically inhibit the potent antiviral activity of A3G.

Regulation of translation represents a critical layer of gene expression control, allowing rapid and localized changes in the expression of proteins in response to extra- and intracellular stimuli. Translational control can occur on a global basis by modifications of the basic translation machinery, or selectively target defined subsets of mRNAs. The latter commonly involves sequence-specific recognition of target mRNAs by trans-acting factors such as miRNA complexes or RBP (RNA-binding protein) (41, 42). To better understand the translational regulation of A3G by Vif, and the role of the two stem-loop structures within the 5'-UTR of A3G mRNA, we searched for cis-acting regulatory elements within this region. Here, we uncovered the importance of a short and conserved uORF (upstream Open Reading Frame) in the distal part (SL2-SL3) of the 5'-UTR of A3G mRNA. Considering that uORFs usually correlate with reduced protein expression of the downstream ORF, we studied the impact of this uORF on A3G translation and on its Vif-mediated translational repression. Extensive mutagenesis of the A3G 5'-UTR and uORF, combined with an analysis of the translational level, indicated that A3G mRNA is translated through a dual leaky-scanning and re-initiation mechanism. Interestingly, disruption of the uORF abrogated the Vif-mediated downregulation of A3G translation. Furthermore, we showed that, in stress conditions, the targeting of A3G mRNA into stress granules was dependent not only on Vif, but also on the presence of the uORF, thus participating to downregulate A3G expression. Taken together, we discovered that human A3G translation is regulated by a small uORF embedded within its 5'-UTR and that HIV-1 Vif uses this specific motif to repress A3G translation and target it to stress granules.

MATERIALS AND METHODS

Plasmids

Plasmid pCMV-hA3G has been previously described (38). Mutated plasmids were generated by Quick-Change Site-directed Mutagenesis (table 1) (Agilent Technology) based on the secondary structure model of the 5'UTR of A3G mRNA (38) and verified by DNA sequencing (Eurofins, Germany). The A3 uORF2 mutants were constructed by inserting a G after the uAUG (translation initiation codon of the uORF) and deleting a G before the uUGA (termination codon of the uORF) in order to place the uUGA in frame with the uAUG, thus changing the wild-type (wt) 23 amino acids sequence MTTRPWEVTLGRAVLKPEAWSRK to MDYEALGGHFREGCPKTRSLE QK. Vif was expressed from pcDNA-hVif expression vector encoding codon-optimized NL4.3 Vif (43) or from

pCRV1-B-LAI (44) expressing Vif from the pLAI.2 strain of HIV-1. Plasmids expressing stress granule (pcDNA GFP-PABP, pcDNA GFP-TIA1) or P-Body (pcDNA GFP-DCP1, pcDNA GFP-AGO2) markers were kindly provided by Dr S. Pfeffer (IBMC-CNRS, Strasbourg).

RACE-PCR

Rapid Amplification of cDNA-ends by PCR (RACE-PCR) was performed following the instructions of the supplier in the 5'/3' RACE Kit, 2nd Generation (Roche). For the 5'-RACE-PCR, 0.2-0.5 µg of human spleen total RNA (Life Technologies) served as template to synthesize the cDNA corresponding to the 5'-end of A3 RNAs by using the Transcriptor Reverse Transcriptase and a specific primer 1 (SP1) according to manufacturer recommendations. The cDNAs were produced for 1 h at 55°C and the reaction was stopped by heating the mixture at 85°C for 5 min. After a purification step, a poly-A tail was added to cDNAs, which were then amplified by a second PCR. This PCR used a dT-Anchor Primer and a second SP2 (0.25 µM each) to amplify 5 µl of polyadenylated cDNAs in a 50 µl mix containing 1 U of Phusion Polymerase, 0.2 mM dNTPs and 1.5 mM $MgCl_2$. The PCR protocol was the following: 3 min at 98°C and 10 cycles of 15 s at 98°C, 30 s at the optimal annealing temperature and 1 min at 72°C. The elongation step was then increased by 20 s steps until it reached 2 min and 23 cycles were performed. A final elongation step of 7 min ended the amplification. A nested PCR was performed with 1 µl of amplicons from the last PCR, in an identical reactional mixture, except for the SP3 used.

For the 3'-RACE-PCR, as mRNAs for the total RNA extract were already polyadenylated, the purification and poly-A tailing steps were not necessary. Using 1 µg of total RNA and a dT-Anchor primer, the cDNAs were synthetized according to the manufacturer protocol and used for a PCR amplification with a PCR Anchor Primer and SP5 primer. Both PCRs were performed as described above. A nested PCR, absent from the initial protocol, was added with a SP6 primer and the same PCR Anchor Primer used in the last PCR to obtain enough material for bacterial transformation.

Cell culture

HEK 293T cells were maintained in Dulbecco's modified Eagle's medium (DMEM, Life Technologies) supplemented with 10% fetal bovine serum (PAA) and 100 U/ml penicillin/streptomycin (Life Technologies) at 37°C and 5% CO_2 atmosphere. Transfections of HEK 293T cells were carried

out using the X-tremeGene 9 DNA Transfection Reagent (Sigma-Aldrich) as recommended by the manufacturer. Briefly, 700,000 cells/well were seeded at 70% confluence in a 6-well plate and co-transfected with 100 ng of pCMV-hA3G constructs and 1 µg of pcDNA-hVif. Cells were also exposed to the chemical proteasome inhibitor ALLN (25 µM) for 14 h.

For FISH and immunofluorescence (IF) experiments, cells were plated on a glass coverslip in 6 well-microplates (700,000 cells/well for HEK 293T cells and 350,000 cells/well for HeLa cells). Cells were cultured in DMEM. Transfections of HEK 293T and Hela cells were carried out as described above. When required, 0.5 µg of stress granules (GFP-PABP or GFP-TIA1) or P-Bodies (GFP-DCP1 or GFP-AGO2) markers were transfected. Twenty-four hours post transfection, stress induction was performed either by treating cells with 500 µM sodium arsenite ($NaAsO_2$, Sigma-Aldrich) or by incubating them at 44°C (heat shock) for 30 min before further analysis.

Immunoblotting

Twenty-four hours post-transfection, cells were washed in PBS 1X (140 mM NaCl, 8 mM NaH_2PO_4, 2 mM Na_2HPO_4) and lysed for 10 min at 4°C in RIPA 1X (PBS 1X, 1% NP40, 0.5% sodium deoxycholate, 0.05% SDS) supplemented with protease inhibitors (complete EDTA Free cocktail, Roche). After 1 h centrifugation at 20,817 g, cell lysates were adjusted to equivalent protein concentration (Bradford assay, Bio-Rad), fractionated on Criterion TGX 4-15% gels (Bio-Rad) and transferred onto 22 µm PVDF membranes using the Trans-Blot Turbo™ Transfer System (Bio-Rad). Blots were probed with appropriate primary antibodies. Polyclonal anti-A3G (#9968), anti-A3H (#12155), anti-A3F (#11226) and monoclonal anti-Vif (#319) antibodies were obtained through the NIH AIDS Research and Reference Reagent Program. Polyclonal anti-A3C (#EB08307) and anti-A3D (#GTX87757) antibodies were obtained from Everest Biotech and Genetex, respectively. Monoclonal anti-□-actin antibody was purchased from Sigma-Aldrich (#A5316). The PVDF membranes were incubated with horseradish peroxidase-conjugated secondary antibodies (Bio-Rad), and the proteins were visualized by enhanced chemiluminescence (ECL) using the ECL Prime Western blotting detection reagent (GE Healthcare) and the ChemiDoc™ Touch Imaging System (Bio-Rad). Bands were quantified using Image J. Student's T-test was used to determine statistical significance.

Real-time qPCR

Twenty-four hours post-transfection, total RNA was isolated from HEK 293T cells using RNAzol®RT (Euromedex). After RNase-free DNase treatment (TURBO DNA-free kit, Invitrogen), total RNA (1 µg) was reverse-transcribed using the iScript™ Reverse Transcription Supermix (Bio-Rad) as recommended by the manufacturer. Subsequent qPCR analysis was performed using the Maxima™ SYBR Green qPCR Master Mix (ThermoFisher) and was monitored on a CFX Real Time System (Bio-Rad). Gene-specific primers were: A3G-fp (forward primer), 5'-GGATCCACCCACATTCACTT-3', and A3G-rp (reverse primer), 5'-ATGCGCTCCACCTCATAAC-3'; □-actin-fp, 5'-GGACTTCGAGCAAGAGATGG-3', and □-actin-rp, 5'-AGCACTGTGTTGGCGTAC AG-3'. The A3G mRNA levels were normalized to those of actin mRNA and relative quantification was determined using the standard curve-based method.

FISH and immunofluorescence (IF) assays

The FISH (Fluorescence In Situ Hybridization) probe was obtained as follow: fragment from nucleotide position 100 to 406 of A3G mRNA was cloned between EcoRI and Xba1 sites into a pcDNA vector. After linearization by XbaI, T7 in vitro transcription was performed in presence of conjugated DIG-11-UTP (Roche) following the manufacturer instruction (1 mM of each dNTP, except dUTP at 0.65 mM and 0.35 mM of the labeled DIG-11-UTP). After DNAse I (Roche) treatment, A3G specific probe was purified by phenol-chloroform extraction and ethanol precipitation. Pellets were resuspended in 50 µl milliQ water giving a 100X concentrated A3G mRNA probe. Aliquots of 1 µl were stored at -80°C.

For FISH and IF (Immuno-Fluorescence) assays, cells were fixed with 4% (w/vol) paraformaldehyde/PBS for 20 min at RT. Fixation was stopped in 100 mM glycine for 10 min at room temperature. Cells were then permeabilized with 0.2% (w/vol) triton X-100/PBS solution at room temperature for 5 min. For FISH assays, after 2 washes in PBS, coverslips were treated for 15 min at room temperature with DNAse I (Roche – 25 U/coverslip) then washed with 1 ml of PBS. One µl of specific A3G mRNA probe was diluted 100x in milliQ water (concentration ~ 5 ng/µl). Coverslips were loaded with 50 µl of pre-warmed hybridization solution (formamide 50%; tRNA 0.1 µg/µl; SSPE 2X (NaCl 300 mM, NaH_2PO_4 20 mM, EDTA 2 mM); Denharts solution 5X (Ficoll 0.1%, Polyvinylpyrrolidone 0.1%, BSA 0.1%); RNAse OUT 0.1 U/µl and 25 ng of specific probe) for 16 h at 42°C, in humid atmosphere. Coverslips were then washed with 50 µl of pre-warmed buffer containing 50% formamide and SSPE 2X for 15 min at 42°C, and then twice with 50 µl SSPE 2X for 5 min at

42°C. Finally, for both FISH and IF assays, after a wash in PBS, coverslips were blocked with 3% (w/vol) BSA in PBS for 1 h at room temperature. Primary antibodies were diluted in 3% (w/vol) BSA/PBS and incubated 3 h at 37°C, followed by incubation of secondary antibodies at room temperature for 2 h in the dark. After a brief wash in PBS, coverslips were mounted in one drop of SlowFade gold antifade reagent (Thermo Fisher) with (IF) or without (FISH) DAPI (Thermo Fisher).

The following primary antibodies were used: sheep polyclonal anti-DIG (Roche); Rabbit polyclonal anti-hA3G-C17 (#10082) and mouse monoclonal anti-HIV-1 Vif (#319) antibodies were obtained through the NIH AIDS Research and Reference Reagent Program. All were used at a $1/500^{e}$ dilution. The following dye-conjugated secondary antibodies were used: Alexa Fluor 647 anti-rabbit, Alexa Fluor 647 anti-goat, Alexa Fluor 488 anti-mouse, Alexa Fluor 546 anti-sheep, Alexa Fluor 405 anti-mouse, Alexa Fluor 594 anti-goat (Life Technologies). All were used at a $1/200^{e}$ dilution.

Microscopy and image analysis

Images were acquired on a Zeiss LSM780 spectral microscope running Zen software, with a 63x,1.4NA Plan-Apochromat oil objective at the IBMP microscopy and cellular imaging platform (Strasbourg, France). Excitation and emission settings were spectrally selected among the 4 laser wavelengths available in the microscope (405; 488; 561; and 633 nm) according to the secondary antibody used. Image processing (contrast, brightness and merges) were performed with ImageJ 1.43m software (45). An additional macro allowing the multichannel profile plot has been designed by Jerome Mutterer from the Microscopy platform. Percentage of cells showing a co-localization between FISH signal (A3G mRNA) and stress or P-Body markers were counted on subsets of 100 cells (n=3).

APOBEC3 genotype data

The NCBI dbSNP database (https://www.ncbi.nlm.nih.gov/snp, July 31st 2019) as well as the UCSC Genome Browser database (https://genome.ucsc.edu/, July 31st 2019) were mined for polymorphic variants in human A3G and A3F mRNA 5'UTRs.

RESULTS

In silico analyses of A3G mRNA 5'UTR identify of a conserved uORF

To further understand the mechanism by which Vif inhibits A3G mRNA in a 5'-UTR-dependent manner (38, 40), we searched for cis-acting elements within the 5'-UTR that could contribute to this repression. Using a computational platform capable of identifying RNA regulatory elements (RegRNA 2.0) (46), we identified a terminal oligopyrimidine (TOP) element that we already excluded from Vif-mediated translational control of A3G mRNA in a precedent study (40) and an uORF within the 5'-UTR of A3G mRNA sequence (Figure 1). uORFs are also cis-regulatory elements that negatively regulate translation of downstream ORF (47–50). In A3G mRNA, our analysis showed that an uORF is encoded within the SL2 and SL3 domains of the 5'-UTR (figure 1). Of note, we previously showed that these two SLs are required for Vif-mediated A3G translation inhibition (40), suggesting this uORF could be involved in this translational inhibition. The uORF is positioned between nucleotides 177 (initiation codon uAUG) and 248 (termination codon uUGA) within the 5'-UTR, 49 nucleotides upstream of the main AUG (mAUG) codon of A3G (nucleotide 298). It encodes a putative peptide of 23 amino acids (figure 1) without any particular motif according to the PROSITE database (https://prosite.expasy.org). We also observed that the Kozak contexts around the upstream and major ORFs are fairly strong (GGGGCCAUGA and CCAAGGAUGA for the uAUG and mAUG, respectively; the initiation codon of translation is underlined), suggesting the uAUG is functional. This uORF is also present in A3F mRNA with 94% and 96% identity at the nucleotide and amino acid level, respectively. To determine if these uORFs are conserved in the human population, we mined the NCBI dbSNP (single nucleotide polymorphism database). In the A3G uORF (+/- 10 nucleotides) region, which included the Kozak context, we did not find any variant with a Minor Allele Frequency (MAF) above 0.005 (table S1). In the A3F uORF region, there was a single common SNP (MAF>0.01, rs35898507) that would induce an amino acid change from G to V in the uORF (G being the ancestral allele present at >96% in the population) (Table S1). Overall, we did not find any variant with a MAF>0.0005 that would dramatically impact the uORFs of A3G and A3F (i.e. that would impact the start codon, the stop codon, or would induce a frameshift). Lastly, the genetic distance between the uORF and the mAUG was also conserved. This shows that herein identified A3G and A3F uORFs are highly conserved in the human population.

The uORF represses translation of A3G mRNA

Since uORFs usually reduce protein expression by approximatively 30-80% (47), we asked whether this motif also regulates A3G mRNA expression. First, we inactivated the uORF of this mRNA by either deleting the whole uORF (A3G ΔuORF), or by substituting the uAUG (A3G suAUG) (figure 2A). The expression of these mutants was examined after transfection of HEK 293T cells and immunoblotting against A3G protein (figure 2B). As expected, uORF inactivation significantly increased A3G protein expression (figure 2B, compare lanes 2-3 to lane 1), suggesting the uORF intrinsically repressed the translation of A3G mRNA.

Next, we wondered whether this translational regulation could be extended to other A3 proteins. Thus, we performed 5'- and 3'-RACE (5'-rapid amplification of cDNA ends analysis) from human spleen total RNA with A3B, A3C, A3D and A3H specific primers (table 2) in order to identify their 5'- and 3'-UTRs (A3A vector (NM_145699.3) was a generous gift from Dr Vincent Caval, Pasteur Institute, Paris; A3F (NM_145298.5) and A3G (NM_021822) were already available in the lab). After cloning and sequencing of the various transformants, corresponding full-length mRNA sequences were synthesized (Proteogenix, France) and consequently cloned into pCMV vectors (figure 3A). The 5'-UTR sequences comprised 44, 106, 407 and 127 nucleotides for A3B, A3C, A3D and A3H, respectively, while their 3'-UTR sequences contained 572, 431, 934 and 372 nucleotides, respectively (figure 3A and table S2). Sequences obtained for the 5'-UTR of A3D and A3H correspond to those published in GenBank™ (accession number NM_152426.3 and NM_001166003.1, respectively). The 5'-UTR sequence of A3B is shorter (44 versus 55 nucleotides) than the reference (NM_004900.4), while the one from A3C is a bit longer (106 versus 103 nucleotides) than the reference (NM_014508.2). All A3 clones were transfected into HEK293T cells in presence or absence of Vif and with or without ALLN (proteasome inhibitor) in order to discriminate the translational inhibition from the proteasomal degradation (40). Our results showed that all A3 proteins are well expressed from full-length mRNA constructs (figure 3B, lanes 2) and are degraded by Vif as expected (figure 3B, lanes 3 and figure 3C, red bars), with the exception of A3A and A3B. This behavior is not unusual for A3A/A3B and could be linked to their Vif-induced nucleocytoplasmic transport (51). A3D was not significantly reduced as previously observed (52). However, in presence of ALLN, we only observed a significant decrease in A3G and A3F expression when Vif was present (figure 3B, compare lanes 4 & 5; figure 3C blue bars), suggesting that these two A3 proteins are the only ones to be regulated at the translational level by Vif. Moreover, sequence analysis of the 5'-UTR of A3A, A3B, A3C, and A3H did

not reveal the presence of any uORF or other regulatory motifs. A short putative uORF (30 nucleotides) is present within the 5'-UTR of A3D (table S2) but was not involved in the Vif-mediated translational inhibition (figure 3B and 3C).

Mechanism of A3G mRNA translation

The results presented above show that the uORF negatively regulates the translation of A3G mRNA. According to the literature (47–50, 53), uORFs can regulate the translation of the main ORF in different manners, in cis or in trans through the encoded peptide, and mechanisms such as leaky-scanning, direct translation initiation at an IRES or re-initiation can be envisaged. To analyze the mechanism of A3G translation, we constructed a series of A3G mRNAs with mutations in the uORF sequence or its surrounding nucleotides and analyzed their expression after transfection of HEK 293T cells (figure 2).

First, we tested the importance of the uORF peptide as a trans-acting element capable of regulating the main ORF translation. To achieve this, we changed the uORF amino acid sequence (see Material & Methods) and studied its effect on A3G expression (mutant A3G uORF2). We observed no effect of the putative peptide in A3G expression (figure 2B, lane 5), consistent with the fact that only in rare cases peptide expressed from an uORF has regulatory effects (54, 55). This result also suggests that the functional importance of the uORF is dependent on features that drive uORF translation rather than the specific peptide produced.

Next, we examined if translation initiation at the uAUG is required for the regulatory mechanism. The frequency of ribosomal recognition of a translation initiation codon is determined by its sequence context (56), and positioning of a translation initiation codon within a "poor" sequence context will result in inefficient ribosomal recognition and bypassing (leaky scanning). We thus replaced the uAUG Kozak consensus sequence (GGGGCCAUGA) by a weak non favorable context (UUUUUUAUGA, mutant A3G WK) (figure 2A). As expected, more ribosomes fail to recognize the uAUG, and we observed a significant increase in protein expression (figure 2B, lane 15), suggesting that the natural uAUG Kozak context is an essential element for the translational repression.

In a natural context of A3G mRNA, the uORF encodes a putative peptide of 23 amino acids. Next, we created a mutant RNA where the translation termination codon of the uORF (suUGA) is inactivated and the uAUG placed in frame with the downstream major ORF (mAUG). Thus, this construct (A3G

suUGA) allows to directly monitor upstream translation initiation, prevent uORF termination and, hence, re-initiation, and downstream translation is only possible by leaky scanning or through a direct entry of the ribosome (IRES - Internal Ribosome Entry Site) at the mAUG. Interestingly, two protein bands can now be observed (figure 2B, lane 4). Indeed, in addition to the standard A3G protein encoded by the main ORF (figure 2B, lane 4, lower band - 384 amino acids), a N-terminally elongated version (424 amino acids) produced by translation initiation at the uAUG can be detected (figure 2B, lane 4, asterisk), demonstrating that the initiation codon of the uORF (uAUG) is functional and in an optimal Kozak context (see above). Moreover, we observed a significant decrease in the expression of the main A3G protein for this mutant (about 50%) (figure 2, lane 4). Since re-initiation is impossible in this case due to the mutated uORF stop-codon, these results strongly suggest that, in the wt situation, A3G is partially expressed by ribosomes re-initiating at the mAUG after having translated the uORF. However, the fact that wt A3G protein is still detected in this mutant also indicates that translation of the main ORF also involves leaky-scanning or IRES-dependent translation.

To test the IRES hypothesis, we inserted a stable stem-loop at the 5'-end of A3G mRNA (figure 2A, mutant A3G-SSL) that prevents binding of the 40S ribosomal subunit and inhibits ribosome scanning (57). However, if an IRES is present within the 5'-UTR of A3G mRNA, ribosomes should load directly on this site and efficiently initiate translation. As observed in figure 2B (lane 14), expression of this mutant was very low, ruling out the hypothesis of an efficient IRES-dependent A3G translation.

To further test the possibility of a re-initiation mechanism, we constructed additional mutants based on previous reports. Indeed, it is well known that re-initiation is more efficient when uORF sequences are small (58) whereas leaky-scanning is not dependent on the length of the uORF (59). Then, reducing the uORF length should enhance A3G expression if a re-initiation mechanism is involved. We thus tested mutants of A3G uORF where the putative 23 amino acids peptide was reduced to 2, 5, 10 or 15 amino acids (figure 2A). The results showed that these mutants significantly decreased (20-40%) A3G protein expression (figure 2B, lanes 6-9), suggesting that the length of the uORF somehow down-regulates the translation of A3G mRNA. To validate this hypothesis and because re-initiation is also dependent on the distance between the stop-codon uUGA and the main AUG of an ORF (inter-ORF region) (59), we then reduced this distance to 24 (mutant A3G Δ249-273) and 6 (mutant A3G Δ249-291) nucleotides by deletions, or by inserting a stop codon at positions 276 (A3G suUGA276) or 289 (A3G suUGA289), thus reducing the inter-ORF region to 21 and 9 nucleotides, respectively (figure

2A). If A3G translation initiation is accomplished by a re-initiation mechanism, reducing this distance should lower protein expression. Interestingly, A3G protein expression was significantly decreased (around 40%) when the inter-ORF region was reduced (figure 2B, lanes 11-13), suggesting that A3G may also be translated through a re-initiation mechanism, except for mutant A3G Δ249-273, which did not show any significant effect on A3G protein expression (figure 2B, lane 10).

To exclude effects of the uORF and mutations on mRNA stability or differential transcription rates, we tested whether the various mutations affect mRNA levels by RTqPCR. None of the mutations significantly impacted RNA stability (figure S1), suggesting that regulation occurs at the translation level.

Initiation at the uORF is required in Vif-mediated A3G translation inhibition

To further characterize the molecular mechanism of Vif-mediated A3G translation inhibition, we seek to determine if the uORF plays a role in this translational repression. We therefore transfected various A3G mRNA mutants in HEK 293T cells in presence or absence of Vif and with or without the proteasome inhibitor ALLN in order to discriminate translational inhibition from proteasomal degradation (40). First, when we co-transfected wt A3G construct with Vif, we observed, as expected, a strong decrease in A3G expression due to a cumulative effect of proteasomal degradation and translation inhibition by Vif (figure 4, red bar, see also figure S2 for western blots), whereas in presence of ALLN, we observed a typical 30-40% reduction in A3G synthesis due to A3G translational repression by Vif (figure 4, blue bar), as previously observed (40). In a second step, we similarly analyzed the effect of Vif (+/- ALLN) on different A3G mRNA constructs. The results showed that A3G ΔuORF mutant presents a strong inhibition of A3G protein expression in presence of Vif (between 60-70%) (figures 4, mutants ΔuORF), similar to wt A3G construct. However, in presence of ALLN, we did not observe any significant decrease in A3G expression when Vif was present (figure 4, blue bars), suggesting that the uORF is required for the Vif-mediated translational inhibition. To validate this hypothesis, we transfected A3G suAUG construct containing a single substitution at the upstream initiation codon. As expected, translational inhibition was not observed with this mutant (figure 4, blue bar).

Finally, we asked whether the inhibition of re-initiation (A3G suUGA) and the peptide nature (A3G uORF2) were important for the translational inhibition of A3G by Vif. These two constructs were

transfected into HEK 293T cells as above and analyze by western blot (figure S2). As expect, A3G proteins expressed from these constructs are degraded through the proteasome in presence of Vif (figure 4, red bars). Interestingly, we showed that both mutants present an expression profile similar to wt A3G in presence of Vif and ALLN (figure 4, blue bars). This suggests that (i) the amino acid sequence (A3G uORF2) is not important for the regulatory translational mechanism, ruling out a possible role of this peptide, in conjunction with Vif, to inhibit A3G translation, and (ii) that Vif inhibits the leaky-scanning mechanism (A3G suUGA).

Taken together, these results indicate that translation initiation at the uORF is essential for the Vif-mediated A3G translational inhibition.

Relocation of A3G mRNA to stress granules is dependent on the uORF and Vif

Mechanisms of translational control dictate which mRNA transcripts gain access to ribosomes, and this process is highly regulated by the interplay of RNA binding proteins (RBPs) and RNA granules, such as processing bodies (P-bodies) or stress granules (SG). SGs are transient foci enriched in translation initiation factors and 40S ribosomal subunits, whereas P-bodies are enriched in RNA-decay machinery. Hence, SGs and P-bodies can be considered as extensions of the messenger ribonucleoprotein (mRNP) translational control cycle, i.e. as compartments where translationally silenced mRNPs are stored (60, 61). Thus, we asked whether Vif can relocate A3G mRNA into these storage compartments and participate to the downregulation of A3G translation, and if so if the uORF plays a role in this process. To test this hypothesis, we analyzed the wt A3G mRNA and two mutant constructs: A3G Δ5'UTR and A3G suAUG. These two mutants (deletion of the 5'-UTR and single substitution of the uAUG) have been chosen because their translation is not down-regulated by Vif ((40) and this study). We began by a careful examination of the intracellular localization of A3G mRNAs and proteins by FISH and immunofluorescence (IF) analysis, respectively, after transfection of HEK 293T cells (figure S3). As expected, wt A3G mRNA and protein were detected in the cytoplasm (figure S3, lane 4). Similarly, mRNAs and proteins expressed from mutants A3G Δ5'-UTR and suAUG were also present in the cytoplasm (figure S3, lanes 5 & 6), suggesting that mutations do not impact on mRNA localization and protein expression.

In a following step, we analyzed the co-localization of A3G mRNAs and proteins with SG and P-body markers in presence or absence of Vif. We co-transfected HEK 293T cells with A3G constructs

in presence or absence of Vif, and then briefly exposed them to arsenite sodium (ARS) or high temperature (44°C) to induce a stress condition. We then performed FISH analysis (A3G mRNAs) and immunofluorescence staining using antibodies directed against Vif and A3G. Stress granule (PABP1 and TIA-1) and P-body (AGO2 and DCP1) marker proteins were expressed as GFP fusion proteins allowing their direct fluorescence detection. First, concerning wt A3G mRNA, we observed as expected that PABP1 was localized into SGs regardless of stress conditions (figure 5A). Interestingly, under stress conditions, while we observed a clear co-localization of A3G and PABP1 proteins into punctate granules in presence or absence of Vif (figure 5A, column 7), co-localization of A3G mRNA and PABP1 was mainly observed in presence of Vif (figure 5A, column 6, yellow dots). We obtained between 50-70% and 45-55% co-localization for PABP1/A3G mRNA (figure 5D, blue bars) and TIA-1/A3G mRNA (figure 5E, blue bars), respectively. Meanwhile, we also performed FISH and IF analysis for A3G Δ5'-UTR (figure 5B) and suAUG (figure 5C) mRNA mutants. Interestingly, whereas a co-localization of A3G and PABP1 proteins was still detected for these two constructs (figure 5B & C, column 7), we observed a significant decrease (around 30%) in the presence of A3G mRNA Δ5'-UTR and suAUG into SGs in the presence of Vif (figure 5D & 5E, red and green bars), suggesting that relocation of A3G mRNA into SGs depends not only on Vif but also on the uORF functionality. Of note, stress conditions alone (44°C or ARS) did not impact on the relocation of the different A3G mRNAs (figure 5D & 5E). Furthermore, we performed similar experiments with P-bodies markers (AGO2 and DCP1) (figure 6). Under physiological conditions, while A3G and AGO2 proteins co-localized (figure 6A, column 7), A3G mRNAs (wt or mutants) are rarely observed co-localizing with P-bodies markers (less than 20% co-localization) regardless of the presence of Vif (figure 6B).

DISCUSSION

The Vif protein is of major importance for an efficient viral infection in non-permissive cells by antagonizing the antiviral activity of A3G proteins. While mechanisms leading to A3G degradation through the recruitment of an E3 ubiquitin ligase complex by Vif are well understood, little is known concerning its translational regulation by Vif. Recently, we showed that the 5'-UTR of A3G mRNA, and specifically the SL2-SL3 domain, was required for the Vif-induced translation inhibition of A3G (40). In the present study, we report that a highly conserved uORF embedded within these structures plays a

crucial role, not only for the repression of A3G translation by Vif, but also for the regulation of its own A3G translation.

Here, by disrupting the uORF (deletion of the uORF or substitution of the uAUG), we showed that translation of A3G was significantly increased (figure 2), indicating that the uORF was indeed a repressive element, as previously observed for several other genes like the tyrosine kinases HCK (Hematopoietic Cell Kinase), LCK (Lymphocyte specific protein tyrosine Kinase), ZAP70 (Zeta chain Associated Protein 70 kDa), YES1 (yes proto-oncogene 1, Src family tyrosine kinase) or the oncogenes MDM2 (Murine Double Minute 2) and CDK4 (Cyclin Dependent Kinase 4) (62). While current data do not suggest that APOBEC3 are oncogenes, recent literature clearly showed that some members of the APOBEC3 family (A3A and A3B for instance) are active on cancer genomes and may impact tumor progression (63). Previous studies found that A3G is overexpressed in patients with diffuse large B-cells leukemia (64) and in pancreatic cancers (65). While cancer development is multifactorial, it is tempting to speculate that cells evolved to limit their expression and that the uORF presence in the 5'-UTR of A3G mRNA may participate to this repression/regulation. Endogenous retroelements, such as ERV, LINE-1, or Alu elements (~42 % of the human genome) (66, 67) are also finely regulated to avoid genetic diseases and cancers (68, 69). Interestingly, APOBEC3 proteins have evolved to protect hosts from the genomic instability caused by retroelements (70) and have been shown to counteract LINE-1 and Alu retrotransposition (71–77). Translational control of mRNA is an important feature of innate immunity but even if the mechanisms remain ill-defined, fine-tuning of their expression must be advantageous for the cell integrity.

uORFs can regulate translation by multiple mechanisms (78, 79). Using mutated A3G mRNA constructs to analyze the impact of the uORF on these various mechanisms, we showed that (i) the distance between the 5'cap and the uORF does not impact on A3G translation (40); (ii) the context around the uAUG is favorable to initiate translation indicating the uAUG is efficiently recognized by the scanning ribosomes but can also be leaky-scanned by the ribosome which will then initiate at the main AUG to express A3G; (iii) A3G may also be translated through a re-initiation mechanism as lengthening the uORF or shortening the intercistronic distance enhances uORF repressive behavior (80–82). In this later case, and as previously observed, the distance between the stop codon and the initiation codon of the main ORF would be too short for the scanning 40S to reacquire a new eIF2•GTP•Met-tRNA^{iMet} complex and initiate translation at the main AUG (83–85). Surprisingly, we did

not observe any increase in A3G expression when we reduced the size of the potentially encoded uORF peptide (figure 2). Indeed, these mutants present a longer intercistronic region (figure 2) and should have benefit from re-initiation. While this mechanism is not fully understood yet, it is possible that the intrinsic sequence of the uORF or its secondary/tertiary structure is of importance for this repression which might be caused by ribosome elongation stalling. While we did not assess the densities of ribosome profiling reads over the 5'UTR of A3G mRNA, we retrieved data from the "Genome Wide Information on Protein Synthesis" website (https://gwips.ucc.ie/) and could observe that uORF was occupied by ribosomes (figure S5A). Interestingly, ribosome occupancy is more pronounced for the second half of the uORF. This suggests they probably stalled during elongation and created a roadblock, hindering the scanning 43S preinitiation complex that bypasses the uORF start codon, which would explain the reduced translation of A3G (a similar profile could be observed for A3F 5'-UTR, figure S5B). Besides, we showed that the nature of the putative 23 amino acids peptide expressed from the uORF (mutant A3G uORF2) has no function in the translational regulation of A3G, reinforcing the importance of the uORF over the peptide sequence.

Furthermore, we showed that the highly structured 5'-UTR of A3G mRNA (38) did not drive any translation through a potential IRES, as the insertion of a stable stem-loop at the 5'-end of the mRNA designed to prevent 43S subunit loading, almost completely inhibited A3G translation (figure 2). Moreover, a genome-wide search yielding a large number of mammalian cellular IRESs did not identify the 5'-UTR of A3G as potential IRES (86). Altogether, these results suggest that A3G is translated through a dual leaky-scanning and re-initiation mechanism. Further studies will be needed to evaluate: (i) the re-initiation efficiency; accurate determination will be difficult as differentiating sole re-initiation from a leaky-scanning/re-initiation mechanism is hard to achieve; (ii) how the ribosome is stalled, through a specific RNA structure or the termination context (87). Studies in mammalian cells and yeast showed that uORF-bearing mRNAs are susceptible to be targeted by NMD which is attributed to the termination events occurring at uORF stop codons (88, 89). This does not seem to be the case for A3G as we did not observe any reduction of wt or mutated mRNA levels (figure S1).

Beyond effects of the uORF on A3G translation, we also observed a link between the presence of a functional uORF and the Vif-mediated translational inhibition of A3G (figure 4). Indeed, under conditions where the proteasomal pathway was inhibited, we showed that Vif was not able to reduce the translation of A3G expressed from mRNA constructs in the absence of a functional uORF (ΔuORF

and suAUG), suggesting that Vif induces A3G translational repression during the initiation steps at the uORF, or that it increases ribosome elongation stalling (figure 4). To the best of our knowledge, the uORF of A3G mRNA would represent the second example (and the first one in vertebrates) for a uORF being co-regulated by a defined protein factor, in addition to SXL (sex lethal protein) that mediates translation inhibition through association to uORF of the Drosophila mls-2 5'-UTR mRNA (90–92). Indeed, in females, msl-2 expression needs to be repressed for viability (dosage compensation), and this repression is achieved by the binding of SXL to uridine stretches in the 5' and 3'UTRs (93, 94). Both mechanisms synergize to achieve full msl-2 translational repression (90). Similarly, multiple mechanisms also exist to inhibit A3G expression through its proteasomal degradation and translational inhibition by Vif. Whereas additional experiments will be needed to clearly decipher this mechanism, one can imagine that Vif interacts with components of the eukaryotic translation initiation machinery to reduce the translational rate of A3G or may recruit cellular factors involved in the negative regulation of the translation (figure 7).

Finally, we observed a strong correlation between the presence and functionality of the uORF on A3G mRNA and its co-localization into SGs in presence of Vif in stress conditions. Indeed, when the uORF was not functional (inhibition of uORF initiation or ΔuORF), the presence of mutated A3G mRNAs was significantly reduced into SGs when Vif was co-expressed (figure 5). However, A3G protein expressed from these constructs can be found into P-bodies and SGs, as previously observed (51, 95–97). The presence of wt A3G mRNA into SGs in presence of Vif is probably not so surprising, since SGs play an important role in the regulation of gene expression at the translational level in response to a variety of external stimuli (98). Therefore, these results validate the notion that the uORF acts as a negative regulator of A3G expression by directing the relocation of A3G mRNA into storage compartments in the presence of Vif (figure 7).

To summarize, we have identified a short uORF within the 5'-UTR of A3G mRNA that is conserved in the human population and drives not only its own translation but is also required by HIV-1 Vif to repress its translation (figure 7). While the relocation into SGs of A3G mRNA by Vif through the uORF could explain in part the downregulation of A3G expression, additional work will be required to firmly establish this mechanism. Deciphering the mechanisms of the Vif-mediated translational inhibition of A3G mRNAs will be important to find new molecular inhibitors able to counteract Vif activity and reduce viral infectivity.

ACKNOWLEDGEMENT

We thank Drs Vincent Caval (Institut Pasteur Paris, France) and Sébastien Pfeffer (IBMC-CNRS, Strasbourg) for kindly providing the APOBEC3A and the different P-body and SG markers, respectively. The following reagents were obtained through the AIDS Research and Reference Reagent Program, Division of AIDS, NIAID, NIH: anti-A3G polyclonal antibody (#9968) from Dr Warner C. Greene, HIV-1 Vif monoclonal antibody (#319) from Dr Michael H. Malim, rabbit anti-human A3F polyclonal antibody (#11226) from Immunodiagnostics, and anti-human A3H monoclonal antibody (P3A3-A10, #12155) from Drs Michael Emerman and Reuben Harris.

FUNDINGS

This work was supported by a grant from the French National Agency for Research on AIDS and Viral Hepatitis (#ECTZ134179) and SIDACTION (#20-1-AEQ-12613-1) to JCP, and by post-doctoral (JB, BS) and doctoral fellowships from ANRS (SG, CL) and the French Ministry of Research and Higher Education (TS, CV). LE is supported by the CNRS and by grants from amfAR (Mathilde Krim Phase II Fellowship #109140-58-RKHF), the ANR LABEX ECOFECT (ANR-11-LABX-0048 of the Université de Lyon, within the program Investissements d'Avenir [ANR-11-IDEX-0007]), the Fondation pour la Recherche Médicale (FRM #ING20160435028), the FINOVI, and the ANRS (#ECTZ19143 and ECTZ118944).

CONFLICT OF INTEREST

None declared.

AUTHOR CONTRIBUTIONS

JCP designed and supervised the project. CL, TS, SG, BS and MW constructed and characterized all A3G mutants by cell transfection and immunoblotting. OG and CV performed the RACE and qRT-PCR, respectively. JB performed FISH and IF experiments. LE performed the genetic analyses of A3G/A3F genes. JCP, RM, AC, and LE analyzed the data. JCP wrote the manuscript with contributions from the other authors. All authors have read and agreed to the published version of the manuscript.

REFERENCES

1. Strebel,K., Daugherty,D., Clouse,K., Cohen,D., Folks,T. and Martin,M.A. (1988) The HIV A (sor) gene product is essential for virus infectivity. *Nature*, **328**, 728–730.
2. Sharma,B., Sharma,M., Daga,M.K., Sachdev,G.K. and Bondi,E. (2007) Effect of omeprazole and domperidone on adult asthmatics with gastroesophageal reflux. *World J. Gastroenterol.*, **13**, 1706–1710.
3. Sakai,H., Shibata,R., Sakuragi,J., Sakuragi,S., Kawamura,M. and Adachi,A. (1993) Cell-dependent requirement of human immunodeficiency virus type 1 Vif protein for maturation of virus particles. *J. Virol.*, **67**, 1663–1666.
4. An,P., Bleiber,G., Duggal,P., Nelson,G., May,M., Mangeat,B., Alobwede,I., Trono,D., Vlahov,D., Donfield,S., *et al.* (2004) APOBEC3G Genetic Variants and Their Influence on the Progression to AIDS. *J. Virol.*, **78**, 11070–11076.
5. Madani,N. and Kabat,D. (1998) An Endogenous Inhibitor of Human Immunodeficiency Virus in Human Lymphocytes Is Overcome by the Viral Vif Protein. *J. Virol.*, **72**, 10251–10255.
6. Simon,J.H.M., Gaddis,N.C., Fouchier,R.A.M. and Malim,M.H. (1998) Evidence for a newly discovered cellular anti-HIV-1 phenotype. *Nat. Med.*, **4**, 1397–1400.
7. Sheehy,A.M., Gaddis,N.C., Choi,J.D. and Malim,M.H. (2002) Isolation of a human gene that inhibits HIV-1 infection and is suppressed by the viral Vif protein. *Nature*, **418**, 646–650.
8. Harris,R.S., Bishop,K.N., Sheehy,A.M., Craig,H.M., Petersen-Mahrt,S.K., Watt,I.N., Neuberger,M.S. and Malim,M.H. (2003) DNA deamination mediates innate immunity to retroviral infection. *Cell*, **113**, 803–809.
9. Malim,M.H. (2009) APOBEC proteins and intrinsic resistance to HIV-1 infection. In *Philosophical Transactions of the Royal Society B: Biological Sciences*.Vol. 364, pp. 675–687.
10. Mangeat,B., Turelli,P., Caron,G., Friedli,M., Perrin,L. and Trono,D. (2003) Broad antiretroviral defence by human APOBEC3G through lethal editing of nascent reverse transcripts. *Nature*, **424**, 99–103.
11. Mbisa,J.L., Barr,R., Thomas,J.A., Vandegraaff,N., Dorweiler,I.J., Svarovskaia,E.S., Brown,W.L., Mansky,L.M., Gorelick,R.J., Harris,R.S., *et al.* (2007) Human Immunodeficiency Virus Type 1 cDNAs Produced in the Presence of APOBEC3G Exhibit Defects in Plus-Strand DNA Transfer and Integration. *J. Virol.*, **81**, 7099–7110.
12. Ooms,M., Brayton,B., Letko,M., Maio,S.M., Pilcher,C.D., Hecht,F.M., Barbour,J.D. and Simon,V. (2013) HIV-1 Vif adaptation to human APOBEC3H haplotypes. *Cell Host Microbe*, **14**, 411–421.
13. Sato,K., Izumi,T., Misawa,N., Kobayashi,T., Yamashita,Y., Ohmichi,M., Ito,M., Takaori-Kondo,A. and Koyanagi,Y. (2010) Remarkable Lethal G-to-A Mutations in vif-Proficient HIV-1 Provirus by Individual APOBEC3 Proteins in Humanized Mice. *J. Virol.*, **84**, 9546–9556.
14. Refsland,E.W., Hultquist,J.F., Luengas,E.M., Ikeda,T., Shaban,N.M., Law,E.K., Brown,W.L., Reilly,C., Emerman,M. and Harris,R.S. (2014) Natural Polymorphisms in Human APOBEC3H and HIV-1 Vif Combine in Primary T Lymphocytes to Affect Viral G-to-A Mutation Levels and Infectivity. *PLoS Genet.*, **10**.
15. Sato,K., Takeuchi,J.S., Misawa,N., Izumi,T., Kobayashi,T., Kimura,Y., Iwami,S., Takaori-Kondo,A., Hu,W.S., Aihara,K., *et al.* (2014) APOBEC3D and APOBEC3F Potently Promote HIV-1 Diversification and Evolution in Humanized Mouse Model. *PLoS Pathog.*, **10**.
16. Alce,T.M. and Popik,W. (2004) APOBEC3G is incorporated into virus-like particles by a direct interaction with HIV-1 gag nucleocapsid protein. *J. Biol. Chem.*, **279**, 34083–34086.
17. Douaisi,M., Dussart,S., Courcoul,M., Bessou,G., Vigne,R. and Decroly,E. (2004) HIV-1 and MLV Gag proteins are sufficient to recruit APOBEC3G into virus-like particles. *Biochem. Biophys. Res. Commun.*, **321**, 566–573.
18. Strebel,K. and Khan,M.A. (2008) APOBEC3G encapsidation into HIV-1 virions: Which RNA is it? *Retrovirology*, **5**.
19. Zennou,V., Perez-Caballero,D., Göttlinger,H. and Bieniasz,P.D. (2004) APOBEC3G Incorporation into Human Immunodeficiency Virus Type 1 Particles. *J. Virol.*, **78**, 12058–12061.
20. Svarovskaia,E.S., Xu,H., Mbisa,J.L., Barr,R., Gorelick,R.J., Ono,A., Freed,E.O., Hu,W.S. and Pathak,V.K. (2004) Human apolipoprotein B mRNA-editing enzyme-catalytic polypeptide-like 3G (APOBEC3G) is incorporated into HIV-1 virions through interactions with viral and nonviral RNAs. *J. Biol. Chem.*, **279**, 35822–35828.
21. Wang,X., Li,X., Ma,J., Zhang,L., Ma,L., Mi,Z., Zhou,J., Guo,F., Kleiman,L. and Cen,S. (2014) Human APOBEC3F incorporation into human immunodeficiency virus type 1 particles. *Virus Res.*, **191**, 30–38.
22. Bishop,K.N., Verma,M., Kim,E.Y., Wolinsky,S.M. and Malim,M.H. (2008) APOBEC3G inhibits

elongation of HIV-1 reverse transcripts. *PLoS Pathog.*, **4**.
23. Iwatani,Y., Chan,D.S.B., Wang,F., Maynard,K.S., Sugiura,W., Gronenborn,A.M., Rouzina,I., Williams,M.C., Musier-Forsyth,K. and Levin,J.G. (2007) Deaminase-independent inhibition of HIV-1 reverse transcription by APOBEC3G. *Nucleic Acids Res.*, **35**, 7096–7108.
24. Mbisa,J.L., Bu,W. and Pathak,V.K. (2010) APOBEC3F and APOBEC3G Inhibit HIV-1 DNA Integration by Different Mechanisms. *J. Virol.*, **84**, 5250–5259.
25. Gillick,K., Pollpeter,D., Phalora,P., Kim,E.-Y., Wolinsky,S.M. and Malim,M.H. (2013) Suppression of HIV-1 Infection by APOBEC3 Proteins in Primary Human CD4 + T Cells Is Associated with Inhibition of Processive Reverse Transcription as Well as Excessive Cytidine Deamination . *J. Virol.*, **87**, 1508–1517.
26. Pollpeter,D., Parsons,M., Sobala,A.E., Coxhead,S., Lang,R.D., Bruns,A.M., Papaioannou,S., McDonnell,J.M., Apolonia,L., Chowdhury,J.A., *et al.* (2018) Deep sequencing of HIV-1 reverse transcripts reveals the multifaceted antiviral functions of APOBEC3G. *Nat. Microbiol.*, **3**, 220–233.
27. Seissler,T., Marquet,R. and Paillart,J.C. (2017) Hijacking of the ubiquitin/proteasome pathway by the hiv auxiliary proteins. *Viruses*, **9**.
28. Yu,X., Yu,Y., Liu,B., Luo,K., Kong,W., Mao,P. and Yu,X.F. (2003) Induction of APOBEC3G Ubiquitination and Degradation by an HIV-1 Vif-Cul5-SCF Complex. *Science (80-.).*, **302**, 1056–1060.
29. Shirakawa,K., Takaori-Kondo,A., Kobayashi,M., Tomonaga,M., Izumi,T., Fukunaga,K., Sasada,A., Abudu,A., Miyauchi,Y., Akari,H., *et al.* (2006) Ubiquitination of APOBEC3 proteins by the Vif-Cullin5-ElonginB-ElonginC complex. *Virology*, **344**, 263–266.
30. Mehle,A., Strack,B., Ancuta,P., Zhang,C., McPike,M. and Gabuzda,D. (2004) Vif Overcomes the Innate Antiviral Activity of APOBEC3G by Promoting Its Degradation in the Ubiquitin-Proteasome Pathway. *J. Biol. Chem.*, **279**, 7792–7798.
31. Hüttenhain,R., Xu,J., Burton,L.A., Gordon,D.E., Hultquist,J.F., Johnson,J.R., Satkamp,L., Hiatt,J., Rhee,D.Y., Baek,K., *et al.* (2019) ARIH2 Is a Vif-Dependent Regulator of CUL5-Mediated APOBEC3G Degradation in HIV Infection. *Cell Host Microbe*, **26**, 86-99.e7.
32. Stanley,B.J., Ehrlich,E.S., Short,L., Yu,Y., Xiao,Z., Yu,X.-F. and Xiong,Y. (2008) Structural Insight into the Human Immunodeficiency Virus Vif SOCS Box and Its Role in Human E3 Ubiquitin Ligase Assembly. *J. Virol.*, **82**, 8656–8663.
33. Bergeron,J.R.C., Huthoff,H., Veselkov,D.A., Beavil,R.L., Simpson,P.J., Matthews,S.J., Malim,M.H. and Sanderson,M.R. (2010) The SOCS-Box of HIV-1 vif interacts with elonginBC by induced-folding to recruit its Cul5-containing ubiquitin ligase complex. *PLoS Pathog.*, **6**.
34. Guo,Y., Dong,L., Qiu,X., Wang,Y., Zhang,B., Liu,H., Yu,Y., Zang,Y., Yang,M. and Huang,Z. (2014) Structural basis for hijacking CBF-β and CUL5 E3 ligase complex by HIV-1 Vif. *Nature*, **505**, 229–233.
35. Kim,D.Y., Kwon,E., Hartley,P.D., Crosby,D.C., Mann,S., Krogan,N.J. and Gross,J.D. (2013) CBFβ Stabilizes HIV Vif to Counteract APOBEC3 at the Expense of RUNX1 Target Gene Expression. *Mol. Cell*, **49**, 632–644.
36. Anderson,B.D. and Harris,R.S. (2015) Transcriptional regulation of APOBEC3 antiviral immunity through the CBF-b/RUNX axis. *Sci. Adv.*, **1**.
37. Stopak,K., De Noronha,C., Yonemoto,W. and Greene,W.C. (2003) HIV-1 Vif blocks the antiviral activity of APOBEC3G by impairing both its translation and intracellular stability. *Mol. Cell*, **12**, 591–601.
38. Mercenne,G., Bernacchi,S., Richer,D., Bec,G., Henriet,S., Paillart,J.C. and Marquet,R. (2009) HIV-1 Vif binds to APOBEC3G mRNA and inhibits its translation. *Nucleic Acids Res.*, **38**, 633–646.
39. Kao,S., Khan,M.A., Miyagi,E., Plishka,R., Buckler-White,A. and Strebel,K. (2003) The Human Immunodeficiency Virus Type 1 Vif Protein Reduces Intracellular Expression and Inhibits Packaging of APOBEC3G (CEM15), a Cellular Inhibitor of Virus Infectivity. *J. Virol.*, **77**, 11398–11407.
40. Guerrero,S., Libre,C., Batisse,J., Mercenne,G., Richer,D., Laumond,G., Decoville,T., Moog,C., Marquet,R. and Paillart,J.C. (2016) Translational regulation of APOBEC3G mRNA by Vif requires its 5′UTR and contributes to restoring HIV-1 infectivity. *Sci. Rep.*, **6**.
41. Jackson,R.J., Hellen,C.U.T. and Pestova,T. V. (2010) The mechanism of eukaryotic translation initiation and principles of its regulation. *Nat. Rev. Mol. Cell Biol.*, **11**, 113–127.
42. Sonenberg,N. and Hinnebusch,A.G. (2009) Regulation of Translation Initiation in Eukaryotes: Mechanisms and Biological Targets. *Cell*, **136**, 731–745.
43. Nguyen,K.L., Llano,M., Akari,H., Miyagi,E., Poeschla,E.M., Strebel,K. and Bour,S. (2004) Codon optimization of the HIV-1 vpu and vif genes stabilizes their mRNA and allows for highly efficient

Rev-independent expression. *Virology*, **319**, 163–175.
44. Binka,M., Ooms,M., Steward,M. and Simon,V. (2012) The Activity Spectrum of Vif from Multiple HIV-1 Subtypes against APOBEC3G, APOBEC3F, and APOBEC3H. *J. Virol.*, **86**, 49–59.
45. Schneider,C.A., Rasband,W.S. and Eliceiri,K.W. (2012) NIH Image to ImageJ: 25 years of image analysis. *Nat. Methods*, **9**, 671–675.
46. Chang TH, Huang HY, Hsu JB, Weng SL, Horng JT,H.H. (2013) RegRNA 2.0. *BMC Bioinformatics*.
47. Calvo,S.E., Pagliarini,D.J. and Mootha,V.K. (2009) Upstream open reading frames cause widespread reduction of protein expression and are polymorphic among humans. *Proc. Natl. Acad. Sci. U. S. A.*, **106**, 7507–7512.
48. Renz,P.F., Valdivia Francia,F. and Sendoel,A. (2020) Some like it translated: small ORFs in the 5′UTR. *Exp. Cell Res.*, **396**.
49. Johnstone,T.G., Bazzini,A.A. and Giraldez,A.J. (2016) Upstream ORF s are prevalent translational repressors in vertebrates . *EMBO J.*, **35**, 706–723.
50. Chew,G.L., Pauli,A. and Schier,A.F. (2016) Conservation of uORF repressiveness and sequence features in mouse, human and zebrafish. *Nat. Commun.*, **7**.
51. Marin,M., Golem,S., Rose,K.M., Kozak,S.L. and Kabat,D. (2008) Human Immunodeficiency Virus Type 1 Vif Functionally Interacts with Diverse APOBEC3 Cytidine Deaminases and Moves with Them between Cytoplasmic Sites of mRNA Metabolism. *J. Virol.*, **82**, 987–998.
52. Hultquist,J.F., Lengyel,J.A., Refsland,E.W., LaRue,R.S., Lackey,L., Brown,W.L. and Harris,R.S. (2011) Human and Rhesus APOBEC3D, APOBEC3F, APOBEC3G, and APOBEC3H Demonstrate a Conserved Capacity To Restrict Vif-Deficient HIV-1. *J. Virol.*, **85**, 11220–11234.
53. Barbosa,C., Peixeiro,I. and Romão,L. (2013) Gene Expression Regulation by Upstream Open Reading Frames and Human Disease. *PLoS Genet.*, **9**.
54. Law,G.L., Raney,A., Heusner,C. and Morris,D.R. (2001) Polyamine Regulation of Ribosome Pausing at the Upstream Open Reading Frame of S-Adenosylmethionine Decarboxylase. *J. Biol. Chem.*, **276**, 38036–38043.
55. Fang,P., Spevak,C.C., Wu,C. and Sachs,M.S. (2004) A nascent polypeptide domain that can regulate translation elongation. *Proc. Natl. Acad. Sci. U. S. A.*, **101**, 4059–4064.
56. Kozak,M. (1987) At least six nucleotides preceding the AUG initiator codon enhance translation in mammalian cells. *J. Mol. Biol.*, **196**, 947–950.
57. Kozak,M. (1989) Circumstances and mechanisms of inhibition of translation by secondary structure in eucaryotic mRNAs. *Mol. Cell. Biol.*, **9**, 5134–5142.
58. Hinnebusch,A.G. (2005) Translational regulation of GCN4 and the general amino acid control of yeast. *Annu. Rev. Microbiol.*, **59**, 407–450.
59. Kozak,M. (2005) Regulation of translation via mRNA structure in prokaryotes and eukaryotes. *Gene*, **361**, 13–37.
60. Guzikowski,A.R., Chen,Y.S. and Zid,B.M. (2019) Stress-induced mRNP granules: Form and function of processing bodies and stress granules. *Wiley Interdiscip. Rev. RNA*, **10**.
61. White,J.P. and Lloyd,R.E. (2012) Regulation of stress granules in virus systems. *Trends Microbiol.*, **20**, 175–183.
62. Wethmar,K., Schulz,J., Muro,E.M., Talyan,S., Andrade-Navarro,M.A. and Leutz,A. (2016) Comprehensive translational control of tyrosine kinase expression by upstream open reading frames. *Oncogene*, **35**, 1736–1742.
63. Green,A.M. and Weitzman,M.D. (2019) The spectrum of APOBEC3 activity: From anti-viral agents to anti-cancer opportunities. *DNA Repair (Amst).*, **83**.
64. Jais,J.P., Haioun,C., Molina,T.J., Rickman,D.S., de Reynies,A., Berger,F., Gisselbrecht,C., Brière,J., Reyes,F., Gaulard,P., *et al.* (2008) The expression of 16 genes related to the cell of origin and immune response predicts survival in elderly patients with diffuse large B-cell lymphoma treated with CHOP and rituximab. *Leukemia*, **22**, 1917–1924.
65. Wu,J., Pan,T.H., Xu,S., Jia,L.T., Zhu,L.L., Mao,J.S., Zhu,Y.L. and Cai,J.T. (2015) The virus-induced protein APOBEC3G inhibits anoikis by activation of Akt kinase in pancreatic cancer cells. *Sci. Rep.*, **5**.
66. Refsland,E.W. and Harris,R.S. (2013) The APOBEC3 family of retroelement restriction factors. *Curr. Top. Microbiol. Immunol.*, **371**, 1–27.
67. Ito,J., Gifford,R.J. and Sato,K. (2020) Retroviruses drive the rapid evolution of mammalian APOBEC3 genes. *Proc. Natl. Acad. Sci. U. S. A.*, **117**, 610–618.
68. Kazazian,H.H., Wong,C., Youssoufian,H., Scott,A.F., Phillips,D.G. and Antonarakis,S.E. (1988) Haemophilia A resulting from de novo insertion of L1 sequences represents a novel mechanism for mutation in man. *Nature*, **332**, 164–166.

69. Morse,B., Rotherg,P.G., South,V.J., Spandorfer,J.M. and Astrin,S.M. (1988) Insertional mutagenesis of the myc locus by a LINE-1 sequence in a human breast carcinoma. *Nature*, **333**, 87–90.
70. Schumann,G.G. (2007) APOBEC3 proteins: Major players in intracellular defence against LINE-1-mediated retrotransposition. In *Biochemical Society Transactions*.Vol. 35, pp. 637–642.
71. Kinomoto,M., Kanno,T., Shimura,M., Ishizaka,Y., Kojima,A., Kurata,T., Sata,T. and Tokunaga,K. (2007) All APOBEC3 family proteins differentially inhibit LINE-1 retrotransposition. *Nucleic Acids Res.*, **35**, 2955–2964.
72. Bogerd,H.P., Wiegand,H.L., Doehle,B.P., Lueders,K.K. and Cullen,B.R. (2006) APOBEC3A and APOBEC3B are potent inhibitors of LTR-retrotransposon function in human cells. *Nucleic Acids Res.*, **34**, 89–95.
73. Chiu,Y.L., Witkowska,H.E., Hall,S.C., Santiago,M., Soros,V.B., Esnault,C., Heidmann,T. and Greene,W.C. (2006) High-molecular-mass APOBEC3G complexes restrict Alu retrotransposition. *Proc. Natl. Acad. Sci. U. S. A.*, **103**, 15588–15593.
74. Bulliard,Y., Turelli,P., Röhrig,U.F., Zoete,V., Mangeat,B., Michielin,O. and Trono,D. (2009) Functional Analysis and Structural Modeling of Human APOBEC3G Reveal the Role of Evolutionarily Conserved Elements in the Inhibition of Human Immunodeficiency Virus Type 1 Infection and Alu Transposition. *J. Virol.*, **83**, 12611–12621.
75. Hulme,A.E., Bogerd,H.P., Cullen,B.R. and Moran,J. V. (2007) Selective inhibition of Alu retrotransposition by APOBEC3G. *Gene*, **390**, 199–205.
76. Koyama,T., Arias,J.F., Iwabu,Y., Yokoyama,M., Fujita,H., Sato,H. and Tokunaga,K. (2013) APOBEC3G oligomerization is associated with the inhibition of both Alu and LINE-1 retrotransposition. *PLoS One*, **8**.
77. McLaughlin,R.N., Gable,J.T., Wittkopp,C.J., Emerman,M. and Malik,H.S. (2016) Conservation and Innovation of APOBEC3A Restriction Functions during Primate Evolution. *Mol. Biol. Evol.*, **33**, 1889–1901.
78. Morris,D.R. and Geballe,A.P. (2000) Upstream Open Reading Frames as Regulators of mRNA Translation. *Mol. Cell. Biol.*, **20**, 8635–8642.
79. Young,S.K. and Wek,R.C. (2016) Upstream open reading frames differentially regulate genespecific translation in the integrated stress response. *J. Biol. Chem.*, **291**, 16927–16935.
80. Andreev,D.E., O'connor,P.B., Fahey,C., Kenny,E.M., Terenin,I.M., Dmitriev,S.E., Cormican,P., Morris,D.W., Shatsky,I.N. and Baranov,P. V. (2015) Translation of 5' leaders is pervasive in genes resistant to eIF2 repression. *Elife*, **2015**.
81. Terenin,I.M., Akulich,K.A., Andreev,D.E., Polyanskaya,S.A., Shatsky,I.N. and Dmitriev,S.E. (2015) Sliding of a 43S ribosomal complex from the recognized AUG codon triggered by a delay in eIF2-bound GTP hydrolysis. *Nucleic Acids Res.*, **44**, 1882–1893.
82. Kozak,M. (2002) Pushing the limits of the scanning mechanism for initiation of translation. *Gene*, **299**, 1–34.
83. Vattem,K.M. and Wek,R.C. (2004) Reinitiation involving upstream ORFs regulates ATF4 mRNA translation in mammalian cells. *Proc. Natl. Acad. Sci. U. S. A.*, **101**, 11269–11274.
84. Harding,H.P., Novoa,I., Zhang,Y., Zeng,H., Wek,R., Schapira,M. and Ron,D. (2000) Regulated translation initiation controls stress-induced gene expression in mammalian cells. *Mol. Cell*, **6**, 1099–1108.
85. Lu,P.D., Harding,H.P. and Ron,D. (2004) Translation reinitiation at alternative open reading frames regulates gene expression in an integrated stress response. *J. Cell Biol.*, **167**, 27–33.
86. Weingarten-Gabbay,S., Elias-Kirma,S., Nir,R., Gritsenko,A.A., Stern-Ginossar,N., Yakhini,Z., Weinberger,A. and Segal,E. (2016) Comparative genetics: Systematic discovery of cap-independent translation sequences in human and viral genomes. *Science (80-.).*, **351**.
87. Wethmar,K. (2014) The regulatory potential of upstream open reading frames in eukaryotic gene expression. *Wiley Interdiscip. Rev. RNA*, **5**, 765–778.
88. He,F., Li,X., Spatrick,P., Casillo,R., Dong,S. and Jacobson,A. (2003) Genome-Wide Analysis of mRNAs Regulated by the Nonsense-Mediated and 5′ to 3′ mRNA Decay Pathways in Yeast. *Mol. Cell*, **12**, 1439–1452.
89. Mendell,J.T., Sharifi,N.A., Meyers,J.L., Martinez-Murillo,F. and Dietz,H.C. (2004) Nonsense surveillance regulates expression of diverse classes of mammalian transcripts and mutes genomic noise. *Nat. Genet.*, **36**, 1073–1078.
90. Medenbach,J., Seiler,M. and Hentze,M.W. (2011) Translational control via protein-regulated upstream open reading frames. *Cell*, **145**, 902–913.
91. Gebauer,F., Merendino,L., Hentze,M.W. and Valcárcel,J. (1998) The Drosophila splicing regulator sex-lethal directly inhibits translation of male-specific-lethal 2 mRNA. *RNA*.

92. Beckmann,K., Grskovic,M., Gebauer,F. and Hentze,M.W. (2005) A dual inhibitory mechanism restricts msl-2 mRNA translation for dosage compensation in Drosophila. *Cell*, **122**, 529–540.
93. Graindorge,A., Militti,C. and Gebauer,F. (2011) Posttranscriptional control of X-chromosome dosage compensation. *Wiley Interdiscip. Rev. RNA*, **2**, 534–545.
94. Duncan,K.E., Strein,C. and Hentze,M.W. (2009) The SXL-UNR Corepressor Complex Uses a PABP-Mediated Mechanism to Inhibit Ribosome Recruitment to msl-2 mRNA. *Mol. Cell*, **36**, 571–582.
95. Gallois-Montbrun,S., Kramer,B., Swanson,C.M., Byers,H., Lynham,S., Ward,M. and Malim,M.H. (2007) Antiviral Protein APOBEC3G Localizes to Ribonucleoprotein Complexes Found in P Bodies and Stress Granules. *J. Virol.*, **81**, 2165–2178.
96. Wichroski,M.J., Robb,G.B. and Rana,T.M. (2006) Human retroviral host restriction factors APOBEC3G and APOBEC3F localize to mRNA processing bodies. *PLoS Pathog.*, **2**, 374–383.
97. Kozak,S.L., Marin,M., Rose,K.M., Bystrom,C. and Kabat,D. (2006) The anti-HIV-1 editing enzyme APOBEC3G binds HIV-1 RNA and messenger RNAs that shuttle between polysomes and stress granules. *J. Biol. Chem.*, **281**, 29105–29119.
98. Kedersha,N.L. and Anderson,P. (2002) Stress granules: sites of mRNA triage that regulate mRNA stability and translatability. *Biochem. Soc. Trans.*, **30**, A117–A117.

Table 1: Description of the primers used in this study

Mutants	Primers	Sequences (5' to 3')
A3G ΔuORF	pS-ΔuORF	GAAGCGGGAGGGGCCAACCCTGGTGCTCCA
	pAS-ΔuORF	TGGAGCACCAGGGTTGGCCCCTCCCGCTTC
A3G suAUG	pS-suAUG	GAAGGGGGAGGGGCCAAGACTACGAGGCCCTGG
	pAS-suAUG	CCAGGGCCTCGTAGTCTTGGCCCCTCCCCCTTC
A3G suUGA	pS-suUGA	GCCTGGAGCAGAAAGGAAACCCTGGTGCTCCA
	pAS-suUGA	TGGAGCACCAGGGTTTCCTTTCTGCTCCAGGC
A3G 2aa	pS-A3G2aa	GCCATGACTACGTGATGATGGGAGGTCACT
	pAS-A3G2aa	AGTGACCTCCCATCATCACGTAGTCATGGC
A3G 5aa	pS-A3G5aa	ACGAGGCCCTGGTGATGAACTTTAGGGAGG
	pAS-A3G5aa	CCTCCCTAAAGTTCATCACCAGGGCCTCGT
A3G 10aa	pS-A3G10aa	GTCACTTTAGGGTGATGAGTCCTAAAACCA
	pAS-A3G10aa	TGGTTTTAGGACTCATCACCCTAAAGTGAC
A3G 15aa	pS-A3G15aa	GCTGTCCTAAAATGATGAGCTTGGAGCAGA
	pAS-A3G15aa	TCTGCTCCAAGCTCATCATTTTAGGACAGC
A3G Δ249-273	pS-Δ249-273	TGGAGCAGAAAGTGATTAGTCGGGACTAGC
	pAS-Δ249-273	GCTAGTCCCGACTAATCACTTTCTGCTCCA
A3G Δ249-291	pS-Δ249-291	TGGAGCAGAAAGTGACCAAGGATGAAGCCT
	pAS-Δ249-291	AGGCTTCATCCTTGGTCACTTTCTGCTCCA
A3G WK	pS-WK	GAAGCGGGAAAAAAAATGGCTACGAGGCCCT
	pAS-WK	AGGGCCTCGTAGCCATAAAAAATCCCGCTTC
A3G uORF2	pS-uORF2	GGGAGGGGCCATGGACTACGAGGCCCTGG
	pAS-uORF2	CCAGGGCCTCGTAGTCCATGGCCCCTCCC
	pS-uORF2	CTTGGAGCAGAAATGAAACCCTGGTGCTCC
	pAS-uORF2	GGAGCACCAGGGTTTCATTTCTGCTCCAAG
A3G uUGA276	pS-uUGA276	CTCCAGACAAAGATCTGATTAGTCGGGACTAGC
	pAS-uUGA276	GCTAGTCCCGACTAATCAGATCTTTGTCTGGAG
A3G uUGA289	pS-uUGA289	TTAGTCGGGACTAGCTGACGGCCAAGGATGAAG
	pAS-uUGA289	CTTCATCCTTGGCCGTCAGCTAGTCCCGACTAA
A3G SSL	pS-SSL	TAGTGAACCGTCAGAAGCTCCACCACGGCCCAAGCTTGGGC CGTGGTGGAGCTCTCTTTCCCTTTGCA
	pAS-SSL	TGCAAAGGGAAAGAGAGCTCCACCACGGCCCAAGCTTGGG CCGTGGTGGAGCTTCTGACGGTTCACTA

Table 2: Description of the primers used for the RACE PCRs

Target Gene	Primer Name	Primer Sequence	Tm
APOBEC3B	A3B SP1	GCA CAG CCC CAG GAG AAG CA	62.7°C
	A3B SP2	GAC CCT GTA GAT CTG GGC CG	59.6°C
	A3B SP3	GGC GCT CCA CCT CAT AGC AC	60.7°C
	A3B SP5	CGG CCC AGA TCT ACA GGG TC	59.6°C
	A3B SP6	ACC AGC AAA GCA ATG TGC TC	56.6°C
APOBEC3C	A3C SP1	GAG ACT CTC CCG TAG CCT TC	56.5°C
	A3C SP2	CAT GAT CTC CAC AGC GAC CC	57.9°C
	A3C SP3	AGA GGC GGG CGG TGA AGA TG	62.3°C
	A3C SP5	GGG TCG CTG TGG AGA TCA TG	57.9°C
	A3C SP6	ATC CAT CCA CCC CCA CAG AC	59.2°C
APOBEC3D	A3DE SP1	CAT TGG GGT GCT CAG CCA AG	59.1°C
	A3DE SP2	AGG TGA TCT GGA AGC GCC TG	59.7°C
	A3DE SP3	CAC ATT TCT GCG TGG TTC TC	54.2°C
	A3DE SP5	TGC AGC CTG AGT CAG GAA GG	59.5°C
	A3DE SP6	TAG AGT GCA ATG GCT GGA TC	55.6°C
APOBEC3H	A3H SP1	AGC GGT TTC TCG TGG TCC AC	60°C
	A3H SP2	TCC ACA CAG AAG CCG CAG CC	63°C
	A3H SP3	GTC AAC CAG CTC CCA GGC AC	61°C
	A3H SP5	GGC TGC GGC TTC TGT GTG GA	63°C
	A3H SP6	GGT CCC GGT GGA GGT CAT GG	62.5°C
	PCR Anchor Primer	GAC CAC GCG TAT CGA TGT CGA C	59.8°C
	dT Anchor Primer	GAC CAC GCG TAT CGA TGT CGA CTT TTT TTT TTT TTT TTV	

FIGURE LEGENDS

Figure 1: Schematic representation of the 5'-UTR of A3G mRNA. The secondary structure of the 5'-UTR of A3G mRNA as determined in (38) is indicated, as well as the TOP element (green) and of the uORF (red). The putative peptide expressed from the uORF is also indicated.

Figure 2: Importance of the uORF for A3G mRNA expression. A) Schematic representation of the different A3G 5'-UTR constructs used in this study. Relative expression of uORF mutants compared to wt A3G mRNA are represented. B) HEK 293T cells were transfected with wt or mutated A3G constructs. Proteins were separated by SDS/PAGE and analyzed by immunoblotting with anti-A3G antibody (#9968). Bands were quantified using Image J and relative expression of A3G is represented in a histogram. Data represent the mean ± S.E.M. for at least three independent experiments. P-values are indicated as follows: *<0.05; **<0.01; ***<0.001; ns: non-significant.

Figure 3: Vif does not inhibit the translation of all APOBEC3 mRNAs. A) Schematic representation of A3 mRNAs identified by RACE-PCR. The lengths of the various 5'- and 3'-UTRs are indicated. B) HEK 293T cells were transfected with plasmids expressing the different A3 proteins in the presence or absence of Vif and in the presence or absence of a proteasome inhibitor (ALLN). Proteins were separated by SDS/PAGE and analyzed by immunoblotting with appropriate antibodies (see Material and Methods) except A3A and A3B which were detected with anti-A3G (#9968) antibody. C) Bands were quantified using Image J and relative expression of A3 proteins is represented. Here, A3+Vif (red bars) and A3G+Vif+ALLN (blue bars) were compared to their equivalent without Vif (lanes 2 and 4) set to 100%, respectively. Data represent the mean ± S.E.M. for at least three independent experiments. P-values are indicated as follows: *<0.05; **<0.01; ***<0.001. ns: non-significant.

Figure 4: Effect of the uORF on Vif-mediated A3G translation inhibition. HEK 293T cells were transfected with plasmids expressing wt and mutated A3G constructs in the presence or absence of Vif and in the presence or absence of a proteasome inhibitor (ALLN). Proteins were separated by SDS/PAGE and analyzed by immunoblotting (see supporting figure 2). Bands were quantified using

Image J and relative expression of A3G proteins is represented. Histograms represent the effects of Vif on A3G: degradation and translation (red bars) and translation only (blue bars). Each condition is compared to the corresponding one without Vif and set to 100% (as above). Data represent the mean ± S.E.M. for at least three independent experiments. P-values are indicated as follows: *<0,05; **<0,01; ns: non-significant.

Figure 5: Importance of the uORF for the relocation of A3G mRNA into stress granules by Vif. HEK 293T cells were transfected with plasmids expressing wt A3G (panel A) as well as Δ5'-UTR (panel B) and suAUG (panel C) mRNAs, in absence or presence of Vif, and with a vector expressing GFP-PABP1 (SG marker). Cells were cultured in various conditions: (i) untreated (no stress) or stressed by (ii) incubation at 44°C or (iii) with arsenite sodium (Ars). Cells were fixed and probed with anti-DIG (A3G mRNAs), anti-A3G (A3G protein), and anti-Vif antibodies. PABP1 and SGs were visualized by direct fluorescence of the GFP-PABP1 fusion protein. Cells were stained with Dapi to visualize nuclei and the images were merged digitally. D) Histograms represent the percentage of co-localization of A3G mRNAs with PABP1 or with TIA (E). Standard deviations are representative for at least three independent experiments. P-values are indicated as follows: **<0,01.

Figure 6: The uORF does not contribute to A3G mRNA relocation to P-bodies by Vif. A) HEK 293T cells were transfected with plasmids expressing wt A3G as well as Δ5'-UTR and suAUG mRNAs, in absence or presence of Vif, and with a vector expressing GFP-AGO2 (P-body marker). Cells were fixed and probed with anti-DIG (A3G mRNAs), anti-A3G (A3G protein), anti-Vif antibodies. AGO2 was visualized by direct fluorescence of the GFP-AGO2 fusion protein. Cells were stained with Dapi to visualize nuclei and the images were merged digitally. B) Histograms represent the percentage of co-localization of A3G mRNAs with AGO2 or DCP1 (another P-body marker). Standard deviations are representative for at least three independent experiments.

Figure 7: Simplified model of A3G mRNA uORF-mediated translational control. A) In absence of Vif, translation of A3G mRNA is controlled by the uORF embedded within its 5'UTR, leading to basal A3G protein translation through leaky-scanning and reinitiation. Ribosome stalling at uORF termination codon is probably participating in reducing A3G yield. **B)** In presence of Vif, the uORF

strengthens the translational inhibition leading to reduced yield of A3G protein. Vif may interact with components of the eukaryotic translation initiation machinery to reduce the translational rate of A3G or recruit cellular factors involved in the negative regulation of the translation. Moreover, relocation of A3G mRNA into storage compartments in presence of Vif participates to the global reduction of A3G level.

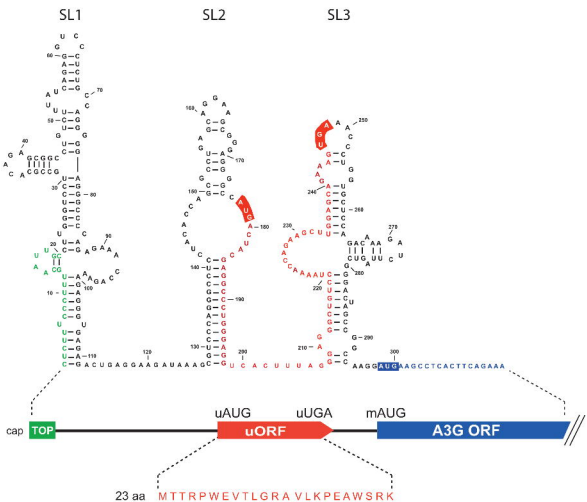
SL1
SL2
SL3
cap
TOP
uAUG
uORF
uGA
mAUG
A3G ORF
23 aa
MTTRPWEVTLGRAVLKPEAWSRK

A

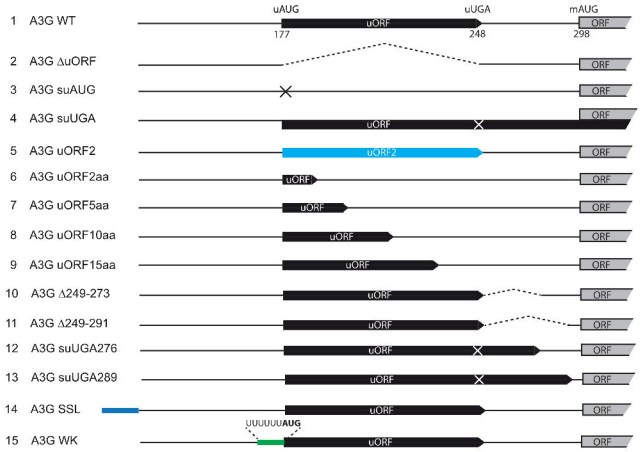
1 A3G WT
uAUG
uORF
uUGA
mAUG
ORF
177
248
298
2 A3G ΔuORF
3 A3G suAUG
4 A3G suUGA
5 A3G uORF2
uORF2
6 A3G uORF2aa
7 A3G uORF5aa
8 A3G uORF10aa
9 A3G uORF15aa
10 A3G Δ249-273
11 A3G Δ249-291
12 A3G suUGA276
13 A3G suUGA289
14 A3G SSL
15 A3G WK
UUUUUUAUG

B

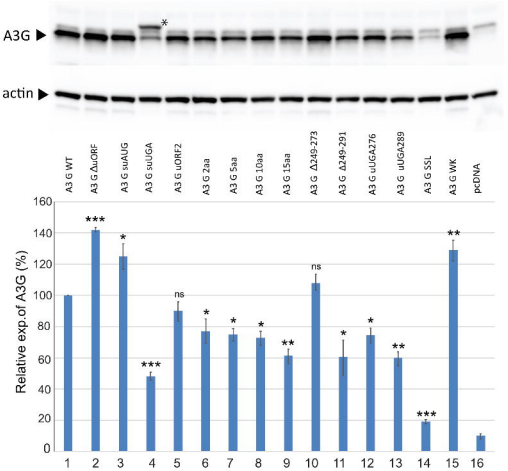
A3G
actin
A3 G WT
A3 G ΔuORF
A3 G suAUG
A3 G suUGA
A3 G uORF2
A3 G 2aa
A3 G 5aa
A3 G 10aa
A3 G 15aa
A3 G Δ249-273
A3 G Δ249-291
A3 G uUGA276
A3 G uUGA289
A3 G SSL
A3 G WK
pcDNA
Relative exp.of A3G (%)
0
20
40
60
80
100
120
140
160
1
2
3
4
5
6
7
8
9
10
11
12
13
14
15
16
***
*
***
ns
*
*
*
**
ns
*
*
**
***
**

A

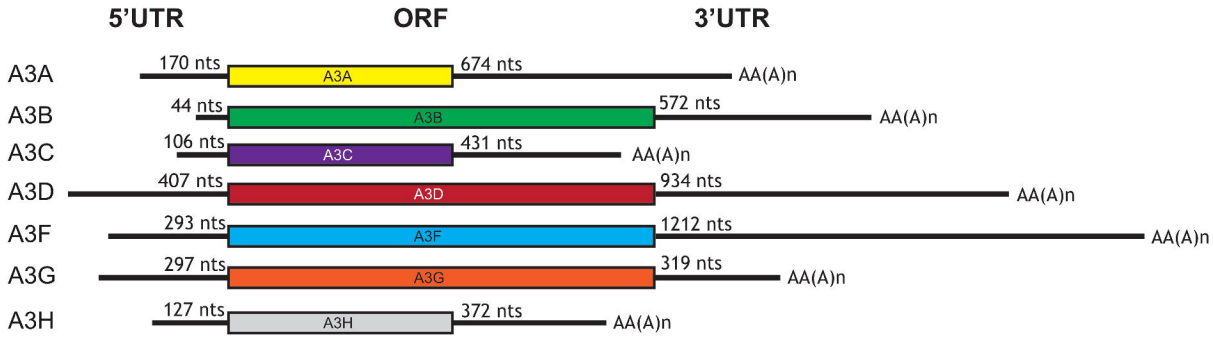

B

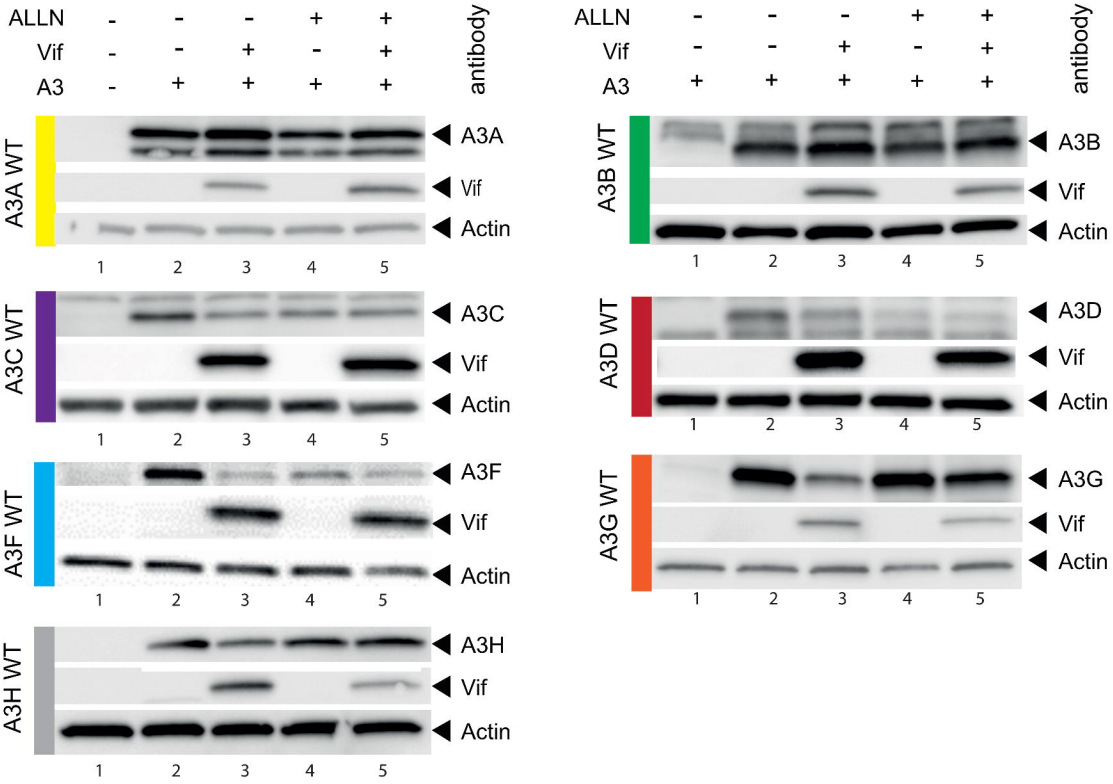

C

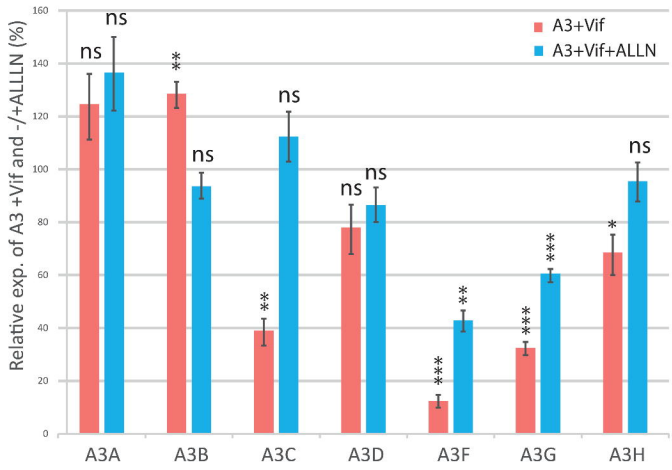

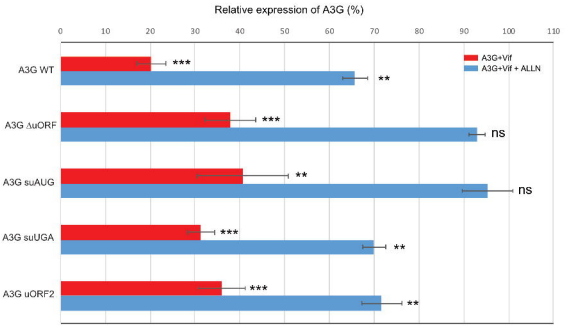
Relative expression of A3G (%)
0
10
20
30
40
50
60
70
80
90
100
110
A3G+Vif
A3G+Vif + ALLN
A3G WT
***
**
A3G ΔuORF
***
ns
A3G suAUG
**
ns
A3G suUGA
***
**
A3G uORF2
***
**

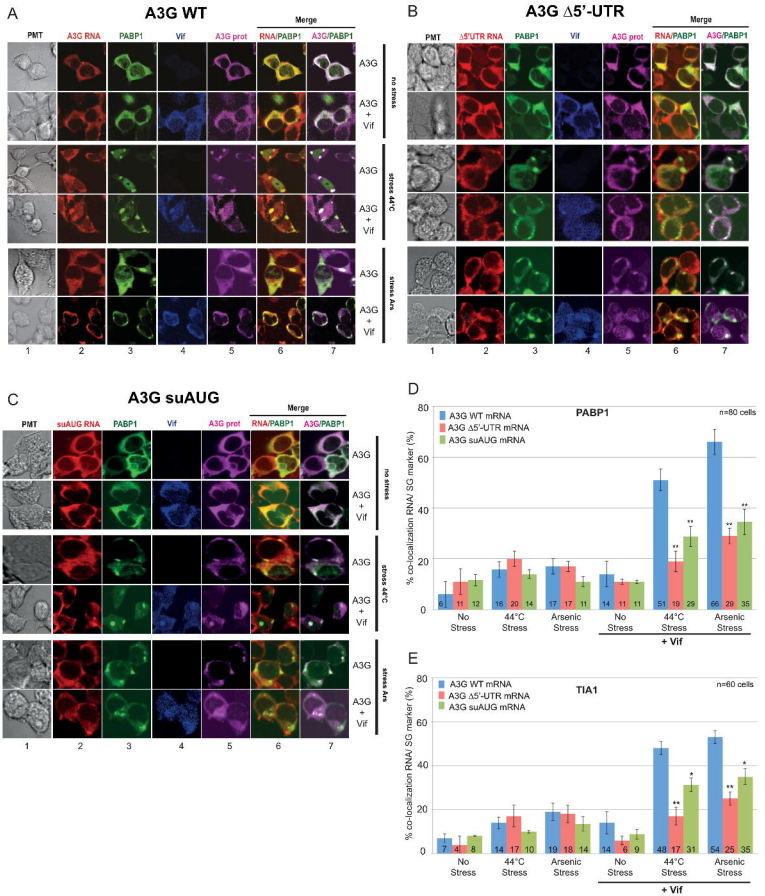
A
A3G WT
PMT
A3G RNA
PABP1
Vif
A3G prot
Merge
RNA/PABP1
A3G/PABP1
A3G
A3G + Vif
no stress
stress 44°C
stress Ars
1
2
3
4
5
6
7
B
A3G Δ5'-UTR
Δ5'UTR RNA
C
A3G suAUG
suAUG RNA
D
PABP1
n=80 cells
A3G WT mRNA
A3G Δ5'-UTR mRNA
A3G suAUG mRNA
% co-localization RNA/ SG marker (%)
6 11 12
16 20 14
17 17 11
14 11 11
51 19 29
66 28 35
No Stress
44°C Stress
Arsenic Stress
+ Vif
E
TIA1
n=60 cells
7 4 8
14 17 10
19 18 14
14 6 9
48 17 31
54 25 35

A

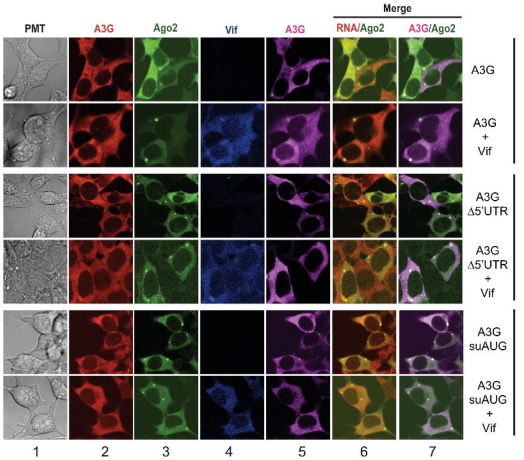
Merge
PMT
A3G
Ago2
Vif
A3G
RNA/Ago2
A3G/Ago2
A3G
A3G + Vif
A3G Δ5'UTR
A3G Δ5'UTR + Vif
A3G suAUG
A3G suAUG + Vif
1
2
3
4
5
6
7

B

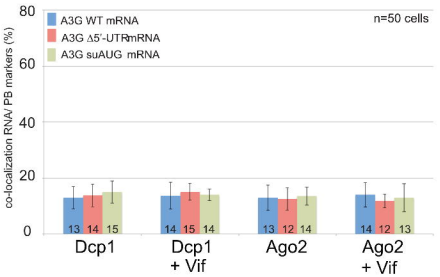
A3G WT mRNA
A3G Δ5'-UTR mRNA
A3G suAUG mRNA
n=50 cells
co-localization RNA/ PB markers (%)
80
60
40
20
0
13 14 15
14 15 14
13 12 14
14 12 13
Dcp1
Dcp1 + Vif
Ago2
Ago2 + Vif

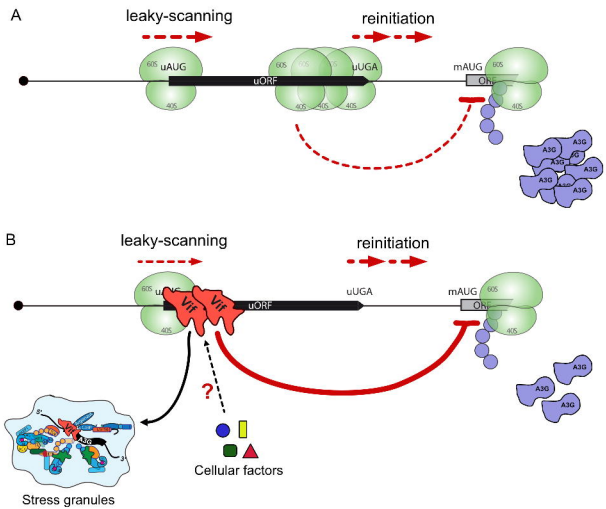
A
leaky-scanning
reinitiation
60S
uAUG
uORF
uUGA
mAUG
ORF
40S
A3G
B
leaky-scanning
reinitiation
Vif
uORF
uUGA
mAUG
ORF
?
Cellular factors
Stress granules